Bulgarian Chemical Communications, Volume 48, Special Issue E (pp. 55 - 63) 2016

Computational modelling of a ground heat exchanger with groundwater flow

Lazaros Aresti[1], Paul Christodoulides[2], Georgios A. Florides[2*]

[1]*Department of Electrical Engineering, Computer Engineering and Informatics, Cyprus University of Technology, Limassol, Cyprus*
[2]*Faculty of Engineering and Technology, Cyprus University of Technology, Limassol, Cyprus*

Multiple layers of ground and the flow of groundwater in some layers have a significant effect on the cooling of vertical heat columns and heat exchangers. This paper investigates the important implication on the design of the Ground Heat Exchanger with regard to their heating effect. For this reason, a thermal model is constructed in COMSOL Multiphysics software and the effect of various parameters such as thermal conductivity of the ground and the groundwater flow velocity is considered. The model parameters were adjusted to present actual (known) parameters of an installed column and were validated against experimental values. The key for an overall capital cost reduction is the borehole length, where the results indicate that by using the groundwater available, construction of shallower Ground Source Heat Pump systems can be achieved with an increase of the coefficient of performance (COP).

Keywords: groundwater flow, Ground Heat Exchanger, multilayer ground

INTRODUCTION

Ground Source Heat Pump (GSHP) systems constitute an evolving technology that has been given significant attention in recent years. GSHP systems have higher energy efficiency and lower environmental impact than regular heat pumps [1]. Geothermal energy, although developed for many years, has not reached a stable and popular state to be widely used. This is due to the high manufacturing and installation cost of Ground Heat Exchangers (GHE) compared to similar, albeit not so effective systems. The capital cost of an air-to-air heat exchanger is lower than that of a GSHP system, although the operation cost is lower for the GSHP system. Only recently the GSHP systems have gained more recognition due to their high efficiency. It is noted that GSHP installations have increased dramatically in recent years (after 2010) with a rate of 10–30% annually [2].

A reliable GSHP system depends on the proper design of the GHE, where the depth reduction is the key to reduce the overall capital cost of a vertical GSHP system. Now, the two most important parameters for designing a GHE are the soil thermal conductivity and the borehole thermal resistance. In its turn, the borehole thermal resistance depends upon the borehole diameter, the pipe size and configuration, the pipe material and the backfill material [3]. In particular, for high soil thermal conductivity and a low borehole thermal resistance, the heat exchange rate will be higher for a given borehole [3]. It is therefore of high importance to determine the thermal characteristics of the ground prior to the system design. For larger installations borehole tests are carried out in a test borehole.

There are several methods available in the literature for the determination of ground thermal characteristics [3], such as soil and rock identification [4], experimental testing of drill cuttings [5], in situ probes [6], and inverse heat conduction models. However, the most commonly used is the Thermal Response Test. The TRT is a method to determine the ground thermal characteristics and it was first introduced by Mogensen in 1983 [7]. TRT is based on heat injection in the borehole at constant power, while the mean borehole temperature is recorded continuously during the test. The recorded fluid temperature response is the temperature developed over time, which is evaluated to obtain the thermal characteristics of the borehole such as the thermal resistance, the volumetric specific heat capacity, and the soil conductivity by using inverse heat transfer analysis [8].

Throughout the years, several analytical and numerical models have been developed to implement fast and reliable predictions of a GHE, where all the models are based on the Fourier's law of heat conduction [9]. The models can be categorized with regard to the type of the 'source' heat (infinite or finite, linear or not) [25]. The most commonly used models are based on: (a) the "infinite line source method," developed by Lord Kelvin [10] and later on applied to the radial heat transfer model by Ingersoll et al. [11], [12]; (b) the "cylindrical heat source method," firstly described

* To whom all correspondence should be sent:
georgios.florides@cut.ac.cy

by Carslaw and Jaeger [13]; (c) the "finite line source method," developed by Eskilson [14] and Claesson and Eskilson [15], which consists of an analytical g-function expression where the solution is determined using a line source with finite length.

Another important aspect to consider when designing a GSHP system is the groundwater flow in the case where an aquifer is present. It must be emphasized that the implementation of the groundwater flow is not adequately supported by current model approaches where overestimates of the thermal conductivities occur as only heat conduction is considered. An indicative case of groundwater flow effect is the in-situ experiment performed in Minnesota [16], where unusually high thermal conductivity values were observed.

The aim of this paper is to study the effect of the groundwater flow on a GHE using a computational modeling approach. The geometry used in this paper (Fig.1) is similar to the one in Florides *et al.* [17] and has been reconstructed by COMSOL Multiphysics v.5.1, which is a computational modelling software allowing the user to use general equations. The user can also add and edit equations manually. It also allows the user to create a CAD model, construct the mesh, apply the physical parameters and post process the results under the same user interface.

MATHEMATICAL MODEL

The heat distribution over time is described by the general heat transfer equation based on the energy balance. For the current application the rate of energy accumulated in the system is equal to the rate of energy entering the system plus the rate of energy generated within the system minus the rate of energy leaving the system [17].

Thus the three dimensional conservation of the transient heat equation for an incompressible fluid is used (and applied in COMSOL Multiphysics) as follows:

$$\rho c_p \frac{\partial T}{\partial t} + \rho_w c_{pw} u \nabla T + \nabla \cdot q = Q \qquad (1)$$

where T is the temperature [K], t is time [s], ρ is the density of the borehole/soil material [kg m^{-3}], c_p is the specific heat capacity of the borehole/soil material at constant pressure [J kg^{-1} K^{-1}], ρ_w is the density of the ground water, c_{pw} is the specific heat capacity of the ground water at constant pressure, u is the velocity of the groundwater [m s^{-1}], Q is the heat source [W m^{-3}] and q is given by the Fourier's law of heat conduction that describes the relationship between the heat flux vector field and the temperature gradient:

$$q = -k\nabla T \qquad (2)$$

where k is the thermal conductivity of the borehole/soil material [W m^{-1} K^{-1}].

In Eq.1, the first term represents the internal energy, the second term is the part of the heat carried away by the flow of water and the third term represents the net heat conducted (as described in Eq.2).

Since the problem will be solved in a transient mode and is time-dependent, the first term is not ruled out as in the case of the steady-state solution. It is worthy to note that in the case where the groundwater is absent, parameter u (velocity) is zero and the second term disappears.

The heat source term describes heat generation within the domain and is set as the heat transfer rate

$$Q = \frac{P_0}{V} \qquad (3)$$

where V is the domain (borehole) volume [m^3] and P_0 is the power [W]. In the case of a single U-tube pipe it is described as

$$P_0 = \dot{m}_w c_{p\,w} dT \qquad (4)$$

where dT is the temperature difference between the inlet and the outlet tubes and $\dot{m}_w$ is the mass flow rate of the water in the tube [kg s^{-1}], defined as

$$\dot{m}_w = \rho_w A_p u_p \qquad (5)$$

where A_p is the area of the tube [m^2] and u_p is the flow velocity in the tubes.

Boundary conditions were set by COMSOL Multiphysics default as "thermal insulation," where there is no heat flux across the boundaries. This setting does not affect the heat distribution along the examined area of the borehole as the domain is set to be significantly larger than the borehole itself.

When water is present in the ground layer, the heat transfer equation in porous media is applied [18] (similar to Eq.1):

$$\rho_{eff} c_{p.eff} \frac{\partial T}{\partial t} + \rho_w c_{pw} u \nabla T + \nabla \cdot q = Q \qquad (6)$$

where $\rho_{eff} c_{p.eff}$ is the volumetric heat capacity of the porous media at constant pressure (ρ_{eff} is the density and $c_{p.eff}$ the specific heat capacity) given by:

$$\rho_{eff} c_{p.eff} = \theta_s \rho_s c_{ps} + (1 - \theta_s) \rho_w c_{pw} \qquad (7)$$

where θ_s is the soil material volume fraction given, ranging from 0 to 1, $\rho_s c_{ps}$ is the volumetric heat capacity of the porous soil material (ρ_s is the density and c_{ps} the specific heat capacity), and, $\rho_w c_{pw}$ is the volumetric heat capacity of the fluid material (water) (being ρ_w the density and c_{pw} the specific heat capacity). The velocity u in the second term of Eq. 6 represents the *Darcy's* velocity as specified in the next section.

The heat conduction q in Eq. 6 can be expressed as:

$$q = -k_{eff}\nabla T \tag{8}$$

where k_{eff} is the effective thermal conductivity that can be calculated by three different methods [19]. The first method, named volume average, assumes that the heat conduction occurs in parallel through the solid material and the fluid (water) and the effective thermal conductivity is expressed as

$$k_{eff} = \theta_s k_s + (1-\theta_s)k_w \tag{9}$$

where k_s is the thermal conductivity of the solid material and k_w is the thermal conductivity of water. The second method considers the heat conduction to occur in series. In this case, the effective thermal conductivity is obtained from the reciprocal average law:

$$\frac{1}{k_{eff}} = \frac{\theta_s}{k_s} + \frac{1-\theta_s}{k_w} \tag{10}$$

The third method calculates the effective thermal conductivity from the weighted geometric mean of the thermal conductivity of both, solid and fluid, materials:

$$k_{eff} = k_s^{\theta_s} k_w^{1-\theta_s} \tag{11}$$

In the current model set-up, the first method of determining the effective thermal conductivity (Eq. 9) was chosen, as it was closer to the requirements of the specific application.

DARCY'S VELOCITY

In order to describe the flow through a porous medium, Darcy's law needs to be applied. The theory was firstly established by Henry Darcy based on experimental results [20] and allows the estimation of the velocity or flow rate within an aquifer. In the investigation of the groundwater effect on the GHE Darcy's velocity is used in the porous media heat transfer equation as stated in Eq. 6.

Darcy's velocity (also called *Specific Discharge*) assumes that flow occurs across the entire cross-section of the soil [21] and is determined as:

$$V_D = -Ki = -K\frac{dh}{L} \tag{12}$$

where K is the hydraulic conductivity [m s^{-1}] that measures the ability for the flow though porous media, i is the hydraulic gradient with dh being the head difference from a datum point [m] and L the distance between the two heads (or boreholes). The minus sign indicates that the flow is moving away from the head. Darcy's velocity is accurately represented though experiments when laminar flow is observed with low Reynolds number [22].

To determine where the Darcy's velocity is applicable the Reynolds number, described below, should be examined:

$$Re = \frac{\rho D V_D}{\mu} \tag{13}$$

where V_D is the discharge velocity or Darcy velocity [m s^{-1}], D is the average soil particle diameter [m], ρ is the density of the fluid [kg m^{-3}] and μ is the dynamic viscosity [kg m^{-1} s^{-1}]. Experiments have shown that the transition from laminar to turbulent conditions occurs approximately at $Re \approx 10$, which is lower than the free flow conditions. The validity of Darcy's law is acceptable at $Re \leq 1$ [22].

As stated in [22], the specific discharge does not predict accurately the flow through a porous media but through a pipe. In order to overcome this issue, the *seepage velocity* was introduced representing the average fluid velocity within the pores and includes a porosity term as described below:

$$v_S = -K\frac{dh}{Ln} = \frac{V_D}{n} \tag{14}$$

where n is the porosity term ($n = A_v/A$) defined as the area of the void space (A_v) through which fluid can flow over the total area (A) of the ground.

COORDINATE SCALING

When modeling a system, as in the present case, it is commonly observed that one of the dimensions may have an enormous difference in relation with the others, and by meshing the model with equilateral cells, high computational memory and time will be required. The way to overcome this difficulty is to scale the large dimension and

balance the coordinate sizes. Consider a coordinate transformation:

$$z = sw \quad (15)$$

where w is the physical coordinate, s is the scaling factor, z is the model coordinate. The general heat equation (Eq. 1 combined with Eq. 2) reads in expanded form (upon substitution of Eq. 15):

$$\rho c_p \frac{\partial T}{\partial t} + \rho c_p u \nabla T + \frac{\partial}{\partial x}\left(k \frac{\partial T}{\partial x}\right) + \frac{\partial}{\partial y}\left(k \frac{\partial T}{\partial y}\right) + s \frac{\partial}{\partial z}\left(s\, k \frac{\partial T}{\partial z}\right) = Q \quad (16)$$

The required physical model has a very large height, 100 m, in contrast with the length and width of the model, which are 10 m and 5 m respectively. Therefore, the model was scaled down on the vertical axis (height). In order to achieve this reduction, the geometry in the COMSOL Multiphysics was built with a scale factor of 0.1 using the thermal conductivity in the materials section. Since multilayer ground is considered, the z-direction thermal conductivity in each layer is scaled as follows:

$$k_z = k(s^2) \quad (17)$$

For the flux conservation and how to un-scale fluxes in scaled models one can refer to [23].

COMPUTATIONAL MODELING

As already mentioned, following the required parameters the model was constructed by COMSOL Multiphysics software. The geometry as seen in Fig.1 was set with two cylinders representing the boreholes. The multilayer ground was constructed with different material properties in order to achieve the required results and the general model, as described in the Coordinate scaling section, was scaled down on the z-axis.

The material properties of each ground layer and the boreholes are described in Table 1 and were taken from the experimental results provided by Florides *et al.* [17]. A simple COMSOL Multiphysics model was validated against the already experimentally validated results of Florides *et al.* [17], giving a good agreement.

Table 1. Material properties

Layer	Height (m)	k (W m^{-1} K^{-1})	C_p (W kg^{-1} K^{-1})	ρ (kg m^{-3})
Top (top)	9×zscale	1.64	2353	731
Region 1	41×zscale	1.73	2290	780
Region 2	30×zscale	1.94	2330	840
Region 3	20×zscale	1.94	2330	840
Bottom	5×zscale	1.94	2330	840
Boreholes	95×zscale	1	800	1500

Subsequently, the groundwater velocity was set using the seepage velocity as described in the previous section, where the hydraulic conductivity is considered for the minimum and maximum values from typical data presented in Domenico and Schwartz [24].

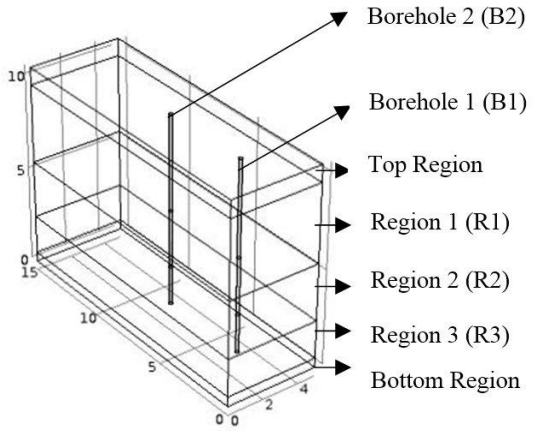

Fig.1. Model Geometry

The value of power used was 2780 W, the same as in Florides *et al.* [17], and the boreholes were set as a heat source with a general source applied of 1275 W m^{-3}. The heat source was not constantly (24 hours) applied as this is not a realistic situation. It was chosen to emit heat for 12 hours, and remain idle for the next 12 hours. To achieve this in COMSOL Multiphysics a rectangle function and an analytic function were selected. Moreover, a heat source applied time function was set (with lower limit 0 and upper limit 12 hours) within the rectangle function. Following on, an argument *t* (time) was introduced in the analytic function (expression of: comp1.rect1(t[1/s]), where rect1 is the rectangle function and comp1 (component) is the location of the function), defining the overall length of 7 days (upper limit) and setting a period of 1 day (periodic extension). For presenting a nearly realistic model, a pulse function was applied, by equating the heat source term to 1 for 12 hours

and to 0 for the next 12 hours, throughout the 7 consecutive days as shown in Fig.2. The analytic function is described graphically in Fig.2. It must be noted that *smoothing* is added by default in COMSOL Multiphysics in order to prevent the equations from shocking, and hence, from producing invalid results.

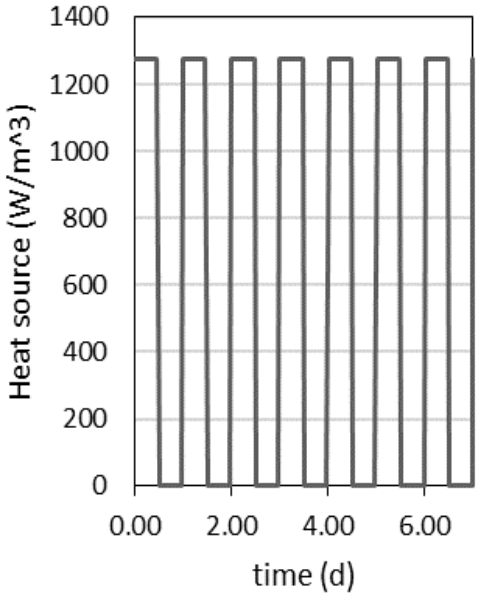

Fig.2. Heat Source analytic function

RESULTS AND DISCUSSION

After the computational model set-up, a set of runs were performed in order to confirm that the scale factor produced reasonable results within acceptable error. The scale comparison was run for the factors of 0.1, 0.2, 0.3 and 0.4. The average temperature on the outer surface of both boreholes in region 3 ground layer (seen in Fig.1) were recorded and analyzed.

The results for all scale factors' values demonstrate a good agreement with less than 0.5 K in temperature difference (Fig.3). These results compare well with professional equipment accuracy, where the tolerance exhibited is usually ±0.2 K. It should be noted that all the parameter values are the same for all 4 cases considered, except the mesh density that had to be changed. The mesh density on the boreholes was maintained at a minimum of 10 to 12 points on the boreholes diameter with a growth rate of 1.2–1.4.

As a consequence, the selected scale factor to proceed with the computational models was 0.1 as it required the least computational time and memory.

The values presented in all the figures are the average surface temperature on the outer wall on region 3 as shown in Fig.1.

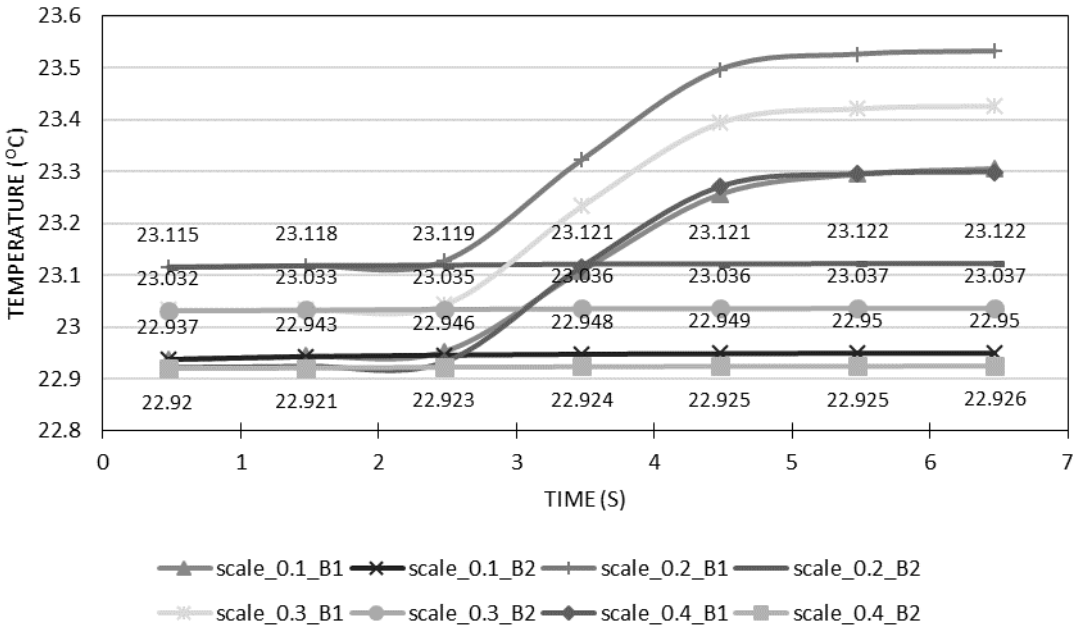

Fig.3. Scale comparison of the region 3 borehole surface showing average temperature over time

Analysis of individual boreholes at different regions allows to observe that the temperature increases with time except in the region of the groundwater (Fig.4). This is due to the fact that groundwater, where is present, dissipates heat away from the borehole. On the contrary, at depths where there is no groundwater, heat is generated and maintained nearby the borehole. In addition, 7 peak points are noticeable due to the pulse function applied. The temperature reaches its peak point each day in the middle of the day after the 12 hours of continuous heat injection.

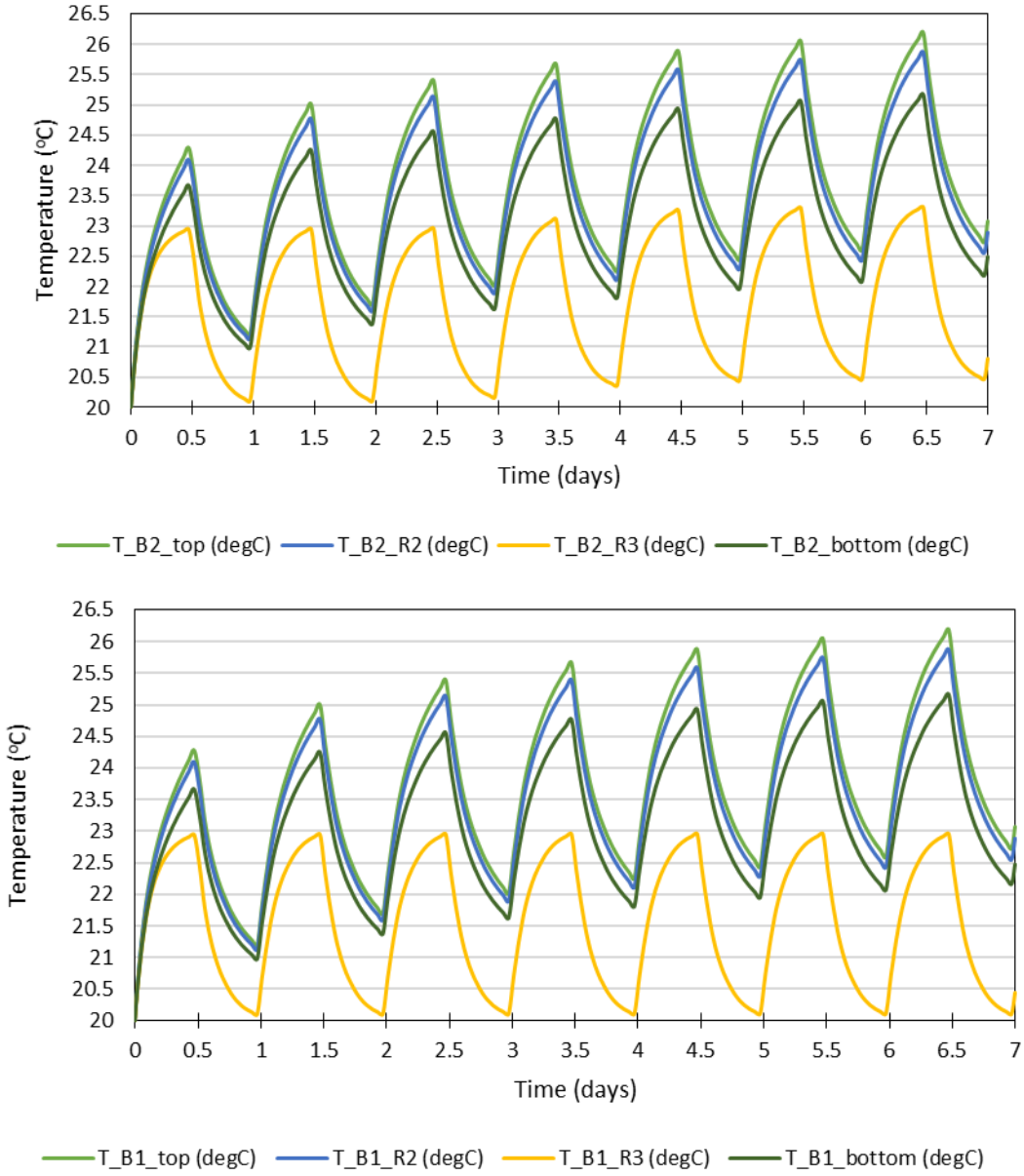

Fig.4. Temperature profiles versus time for a seepage velocity vS = 10^{-5} m s^{-1} for Borehole 1 (B1-upstream) and Borehole 2 (B2-downstream)

It is easier to examine the rise of the heat by plotting only the maximum points in each borehole (Fig.5 and Fig.6). In Fig.5 it can be observed that by increasing the groundwater velocity (seepage velocity as applied in the model) the average surface temperature on the groundwater region decreases. It is noteworthy that when low seepage velocity values are applied (v_S=1.6667×10^{-9} and v_S=10^{-9}), the model generates the same temperature peak points (see plots).

Thus, it can be concluded that when seepage velocity is smaller than 10^{-9}, it is not enough to cool down the boreholes, whereas under maximum seepage velocity regime, the boreholes show a lower average temperature and reach steady state in a shorter time. It is also noticeable that in the first borehole, the average temperature reaches a steady state the first day, whereas in the second borehole (downstream) there is an increase in temperature before it reaches steady state again the fourth day.

In order to further examine the temperature increasing in the second borehole, a direct comparison between the two boreholes, under the same conditions, is shown in Fig.7. The heat carried away from the first borehole interferes with the second borehole when the groundwater velocity is high enough – like in the case of the maximum seepage velocity (v_S = 10^{-5} m s^{-1}) – as can be observed in 2D y-z and x-y plots (Fig.8 and Fig.9).

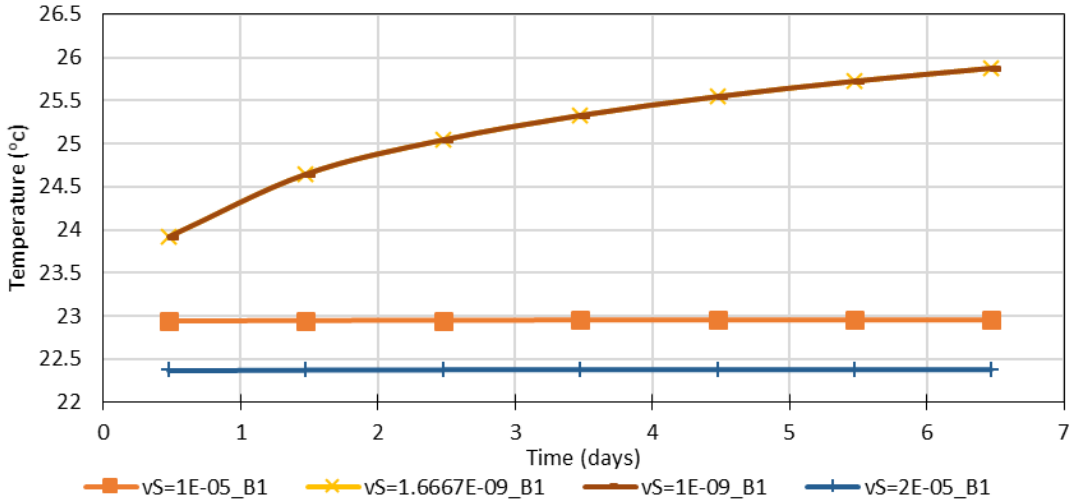

Fig.5. Temperature peak points versus time for borehole 1 (B1) in region 3 for various values of seepage velocity (v_S)

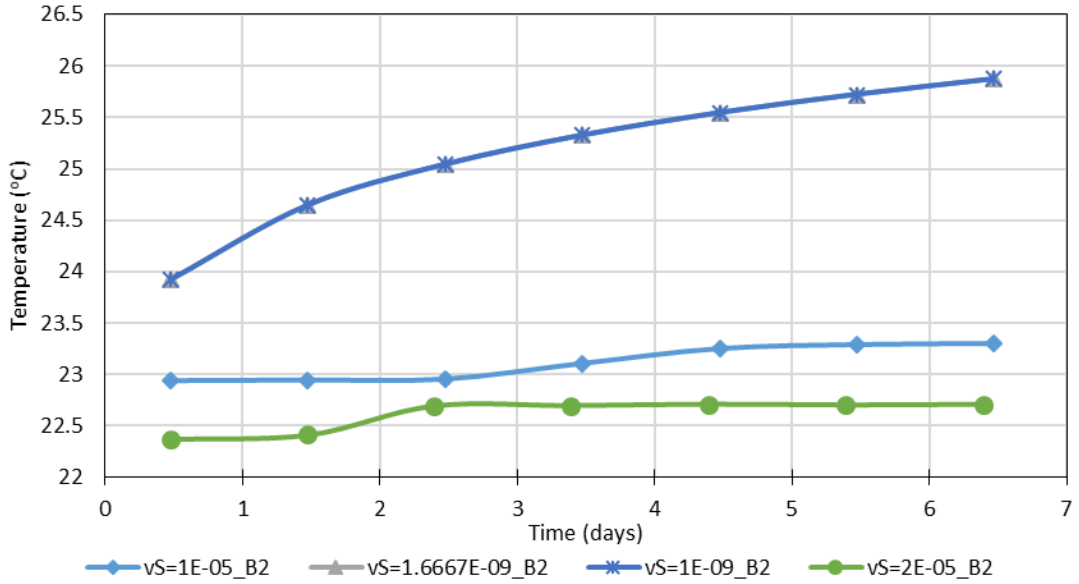

Fig.6. Temperature peak points versus time for borehole 2 (B2) in region 3 for various values of seepage velocity (v_S)

This interference occurs after 60 hours and continues for another 3 days until the heat flow is steady and the average surface temperature on the second borehole reaches steady state.

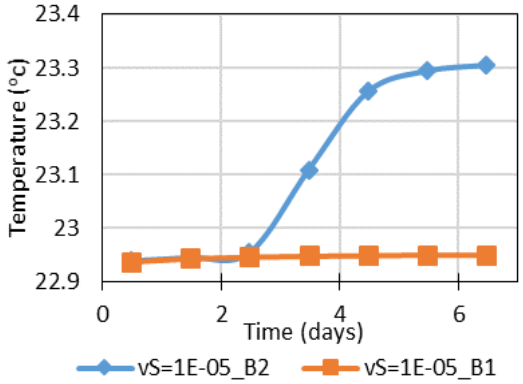

Fig.7. Temperature peak points at vS = 10^{-5}ms^{-1} versus time for both boreholes in region 3

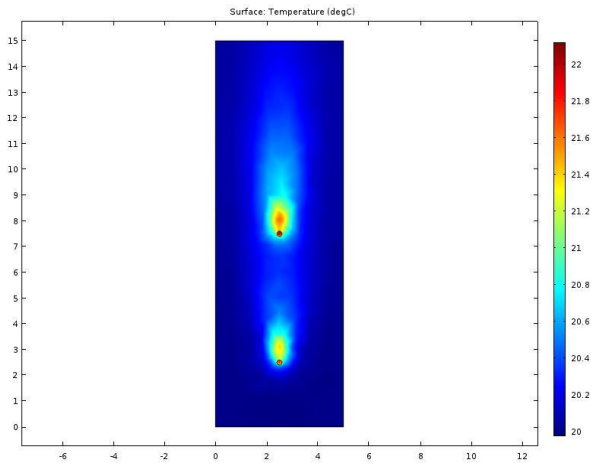

Fig.8. 2D cut-plane on the x-y plane, vS = 10^{-5} m s^{-1}, t = 7 days, center of region 3

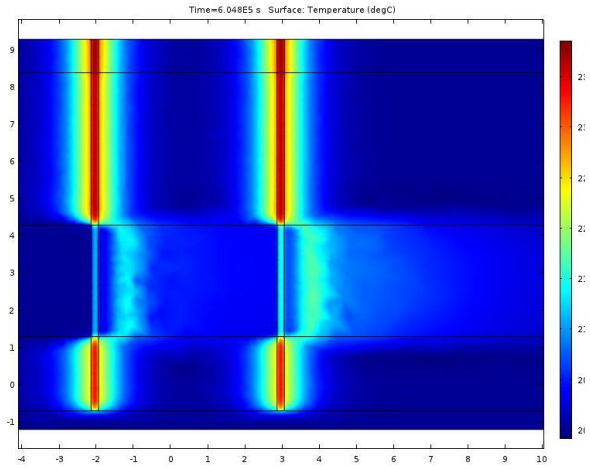

Fig.9. 2D cut-plane on the y-z plane, vS = 10^{-5} m s^{-1}, t = 7 days, center of boreholes

The effect of the interference, when the maximum hydraulic conductivity is applied, can also be noticed by plotting the isothermal contours. After a 2 days run the isothermal contours of the first borehole have not reached the second borehole (Fig.10). After a 5 days run (Fig.11), the first borehole interferes with the second borehole, whence the increased temperature detected.

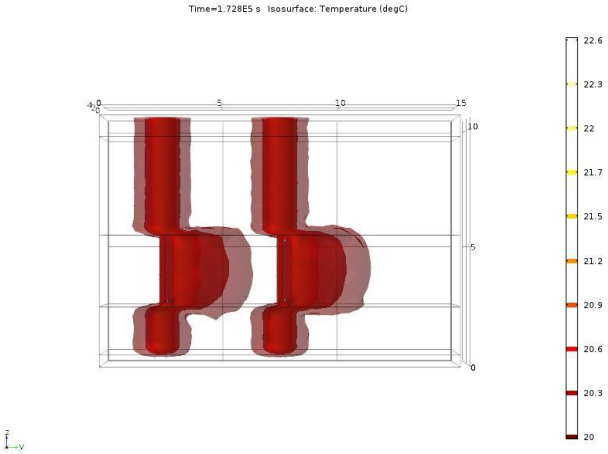

Fig.10. Isothermal contours, vS = 10^{-5} m s^{-1}, t = 2 days

As can be clearly seen in Fig.12, the interference does not occur at lower velocities (e.g. vS = 1.6667×10–9 m s–1 for minimum hydraulic conductivity applied) as expected due to the low velocity in the groundwater region. Of course, even this very low seepage velocity can still produce lower average surface temperature in region 3 that in the other regions (as seen in Fig.4). Note that steady state has not been reached after 7 days of computational run (Fig.5 and Fig.6), as in the case of the higher seepage velocity applied (vS = 10–5 m s–1 for maximum hydraulic conductivity).

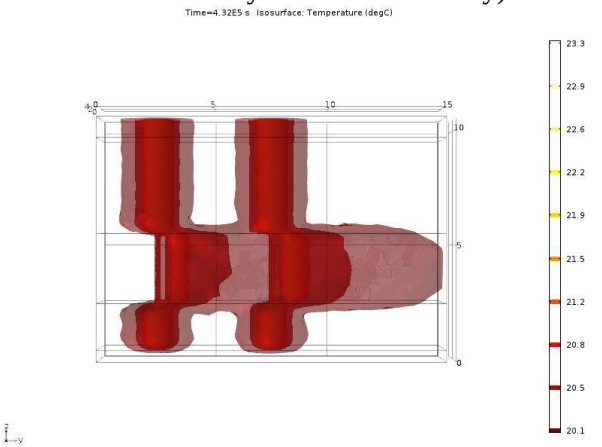

Fig.11. Isothermal contours, $v_S = 10^{-5}$ m s^{-1}, t=5 days

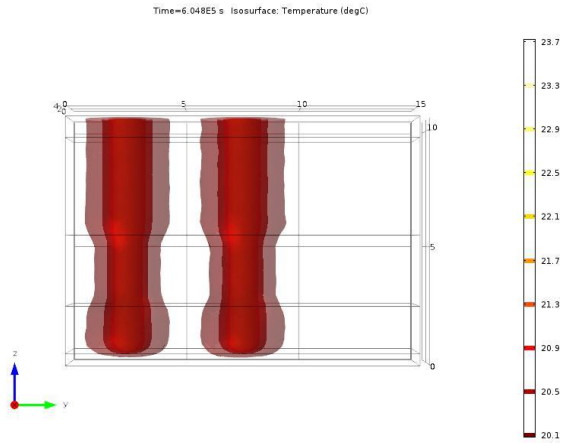

Fig.12. Isothermal contours, vS = 1.6667×10^{-9} m s^{-1}, t = 7 days

CONCLUSIONS

In this paper the effect of the groundwater flow on a GHE in cooling mode has been examined through computational modeling using COMSOL Multiphysics software. Heat transfer in porous media, Darcy's velocity and seepage velocity were introduced by taking typical values of hydraulic conductivity and were adapted in COMSOL Multiphysics. The coordinate scaling technique was employed in order to save valuable computational time and memory. The heat source was added to the model as a pulse function and it was activated 12 hours a day.

Moreover, the average borehole surface temperatures on every ground layer were presented for low and high seepage velocities. The results indicate that groundwater flow has an effect on the average surface temperature, and in the water-bearing layer the average temperature decreases as

opposed to the dry regions. It is also noticeable that the temperature of the affected ground layer reaches a steady-state much sooner than in other regions. Additionally, when the groundwater flow velocity is high, the two boreholes are observed to interfere with each other. This interference has an effect on the downstream borehole that can reach a lower steady-state temperature.

Further examination of cooling and heating mode must be considered in the future and in addition, in-situ experiments could be conducted in order to validate directly the model using a groundwater flow GHE.

REFERENCES

1 Y. Xiaohui, Z. Yufeng, D. Na, W. Jianshuan, Z. Dongwen and W. Jilin, "Thermal response test and numerical analysis based on two models for ground-source heat pump system," *Energy and Buildings*, vol. 66, pp. 657-666, 2013.

2 H. Yang, P. Cui, Z. Fang, "Vertical-borehole ground-coupled heat pumps: A review of models and systems," *Applied Energy*, vol. 87, no. 1, pp. 16-27, 2010.

3 Z. Changxing, G. Zhanjun, L. Yufeng, C. Xiaochun and P. Donggen, "A review on thermal response test of ground-coupled heat pump systems," *Renewable and Sustainable Energy Reviews*, vol. 40, no. 851-867, 2014.

4 J. Bose, "Soil and rock classification for design of ground coupled heat pump systems-field manual," Electric Power Research Institute, 1989.

5 J. Sass, A. Lachenbruch and R. Munroe, "Thermal conductivity of rockes from measurments on fragments and its application to heat flow determinations," *J Geophys Res*, vol. 76, pp. 3391-401, 1971.

6 A. Choudhary, "An approach to determine the termal conductivity and diffusivity of a rock in situ.," Oklahoma State University, 1976.

7 P. Mogensen, "Fluid to Duct Wall Heat Transfer in Duct System Heat Storage," Stockholm. Sweden, 1983.

8 S. Gehlin, "Thermal response test: method development and evaluation.," Sweden, 2002.

9 G. Florides and S. Kalogirou, "Ground heat exchanges - A review on systems, models and applications," *Reneable energy*, vol. 32, no. 15, p. 2461–2478, 2007.

10 T. Kelvin, Mathematical and physical papers. London: Cambridge University Press, 1882.

11 L. Ingersoll, O. J. Zobel and A. C. Ingersoll, Heat conduction with engineering, geological and other applications., New York: McGraw-Hill, 1954.

12 L. Ingersoll, F. Adler, H. Plass and A. Ingersoll, "Theory of earth heat exchangers for the heat pump," *ASHVE Trans*, vol. 56, pp. 167-88, 1950.

13 H. Carslaw and J. Jaeger, Conduction of heat in solids, 2nd ed., Oxford, UK: Oxford University Press, 1959.

14 P. Eskilson, "Thermal analysis of heat extraction boreholes," University of Lund, Lund, Sweden, 1987.

15 J. Claesson and P. Eskilson, "Conductive heat extraction by a deep borehole," Sweden, 1988.

16 C. Remund, Personal communication., Northern Geo- thermal Support Center: South Dakota State University, Brookings, South Dakota, 1998.

17 G. Florides, E. Theofanous, I. Iosif-Stylianou, S. Tassou, P. Christodoulides, Z. Zomeni, E. Tsiolakis, S. Kalogirou, V. Messaritis, P. Pouloupatis and G. Panayiotou, "Modeling and assessment of the efficiency of horizontal and vertical ground heat exchangers," *Energy*, vol. 58, pp. 655-663, 2013.

18 J. Bear and Y. Bachmat, Introduction to Modeling of Transport Phenomena in Porous Media, vol. 4, Springer Science & Business Media, 1990.

19 D. Nield and A. Bejan, Convection in Porous Media, in Convection Heat Transfer, Fourth Edition, Hoboken, NJ, USA: John Wiley & Sons, Inc., 2013.

20 H. Darcy, Les Fontaines Publiques de la Ville de Dijon, Paris: Dalmont, 1856.

21 A. D. Chiasson, S. J. Rees and J. D. Spitler, "Preliminary assessment of the effects of groundwater flow on closed-loop ground-source heat pump systems," *ASHRAE Transactions*, vol. 106, no. 1, pp. 380-393, 2000.

22 M. E. Harr, Groundwater and Seepage, New York: Dover Publication Inc, 1990.

23 P. S. Inc, "FlexPDE user guide," 2010. [Online]. Available: http://www.pdesolutions.com/help/index.html?coordinatescaling.html. [Accessed Nov 2015].

24 P. Domenico and F. Schwartz, Physical and chemical hydrogeology, New York: John Wiley & Sons, 1990.

25 S. Javed, P. Fahlén and J. Claesson, "Vertical ground heat exchangers: A review of heat flow models.," in *Proceedings vol. CD-proceedings*, Stockholm, Sweden, 2009.